

## Targeted deletion of all isoforms of the *trkC* gene suggests the use of alternate receptors by its ligand neurotrophin-3 in neuronal development and implicates *trkC* in normal cardiogenesis

LINO TESSAROLLO\*<sup>†‡</sup>, PANTELIS TSOUFAS<sup>†§</sup>, MICHAEL J. DONOVAN<sup>¶</sup>, MARY ELLEN PALKO\*<sup>†</sup>, JANET BLAIR-FLYNN\*<sup>†</sup>, BARBARA L. HEMPSTEAD<sup>||</sup>, AND LUIS F. PARADA<sup>†\*\*</sup>

\*Neural Development Group and <sup>†</sup>Molecular Embryology Section, ABL-Basic Research Program, National Cancer Institute–Frederick Cancer Research and Development Center, Frederick, MD 21702; <sup>‡</sup>Department of Pathology, Children's Hospital, Boston, MA 02115; and <sup>§</sup>Department of Medicine, Cornell University Medical College, New York, NY 10021

Communicated by Rodolfo R. Llinas, New York University Medical Center, New York, NY, September 29, 1997 (received for review May 19, 1997)

**ABSTRACT** We have generated null mutant mice that lack expression of all isoforms encoded by the *trkC* locus. These mice display a behavioral phenotype characterized by a loss of proprioceptive neurons. Neuronal counts of sensory ganglia in the *trkC* mutant mice reveal less severe losses than those in *NT-3* null mutant mice, strongly suggesting that *NT-3*, *in vivo*, may signal through receptors other than *trkC*. Mice lacking either *NT-3* or all *trkC* receptor isoforms die in the early postnatal period. Histological examination of *trkC*-deficient mice reveals severe cardiac defects such as atrial and ventricular septal defects, and valvular defects including pulmonic stenosis. Formation of these structures during development is dependent on cardiac neural crest function. The similarities in cardiac defects observed in the *trkC* and *NT-3* null mutant mice indicate that the *trkC* receptor mediates most *NT-3* effects on the cardiac neural crest.

Neurotrophins are members of a highly homologous family of growth factors that contribute to the regulation of proliferation, survival, and differentiation of different cell populations in the mammalian nervous system (1). This family consists of nerve growth factor (NGF), brain derived neurotrophic factor (BDNF), neurotrophin-3 (NT-3), neurotrophin-4/5, and neurotrophin-6 (2, 3). Upon binding to extracellular Ig-like domains of the Trk receptor tyrosine kinases, neurotrophins activate these receptors, thus triggering subsequent biological responses (4, 5). Neurotrophins also interact with the p75 neurotrophin receptor that lacks intrinsic enzymatic activity (6, 7).

*In vitro* experiments have demonstrated that NGF binds only to *trkA* (8), and BDNF and neurotrophin-4/5 bind to *trkB* (9–11). NT-3 binds and signals mainly through *trkC* (12) but can bind also to *trkA* and *trkB* with lower affinity in biochemical assays (5). NT-3 is also able to activate the *trkA* and *trkB* receptors in NIH 3T3 cells (13). However, physiological concentrations of NT-3 fail to activate *trkA* and *trkB* when these receptors are coexpressed in neural crest-derived cells (PC12 cells) (13). Thus, it has been hypothesized that NT-3-mediated signals in neurons are transmitted specifically by *trkC* (13).

The pattern of expression of neurotrophins and their receptors in adult and embryonic tissues in rodents, in combination with *in vitro* and *in vivo* assays, have helped to predict the cells within sensory and motor ganglia likely to be the targets of neurotrophin action (14–16). In dorsal root ganglia (DRG), correlations have been made between the expression of *trk*

receptors on different soma size neurons and target tissue innervation; cutaneous afferents correlate with small neurons that are *trkA* positive and muscle afferents correlate with large *trkC*-expressing neurons (16, 17). However, these studies also suggest that different neurotrophins may act on a single neuronal population during different stages of development. For example, before the axons reach their target fields, neurotrophins may exert local effects (18). Upon reaching their target field, neurons then switch dependence to a different neurotrophin (19, 20). Also, individual neurons can express more than one type of *trk* receptor, suggesting that neurotrophins could have additive or independent functions on the same cell (17, 21, 22). Furthermore, the wide expression of *trkC* in many mouse embryonic tissues suggests that NT-3 could have pleiotropic functions during development affecting both neuronal and nonneuronal tissues (23).

Mice lacking individual members of the neurotrophin and *trk* receptor families have confirmed some of these early hypotheses. In particular, *NGF*- and *trkA*-deficient animals have similar neuronal deficits, hypoalgesia, and reductions in the number of small-diameter nociceptive afferents (24, 25). Although *BDNF* and *trkB* null mutant animals also exhibit similar deficits, their analysis is complicated by an additional ligand for *trkB*, neurotrophin-4/5, as well as the persistent expression of truncated isoforms of the *trkB* receptors (25–29).

The mammalian *trkC* locus encodes at least eight polypeptides (30, 31). Three of these proteins represent tyrosine kinase receptors that differ in insertions in the kinase domain; the other receptors lack the catalytic kinase domain. It is not clear whether the truncated isoforms can signal or exert effects on *trkC*-kinase receptors. The survival and neuronal deficits in *NT-3*  $-/-$  and mice that lack only the kinase active isoforms of *trkC* (*trkC*-kinase  $-/-$ ) are quite different even though both exhibit similar deficiencies in movement and loss of large-diameter muscle afferents projecting to the ventral horn (32–36). The majority of the *NT-3*-deficient animals die just after birth, whereas the *trkC*-kinase  $-/-$  animals survive up to 3 weeks. Neuronal counts on spinal sensory ganglia show that the loss of neurons is greater in *NT-3*  $-/-$  than in *trkC*-kinase  $-/-$  mice (32–34). To address these discrepancies between *NT-3* and *trkC*-kinase deficient mice, we have generated and

Abbreviations: NGF, nerve growth factor; BDNF, brain-derived neurotrophic factor; NT-3, neurotrophin-3; DRG, dorsal root ganglia.

<sup>‡</sup>To whom reprint requests should be addressed at: ABL-Basic Research Program, National Cancer Institute–Frederick Cancer Research and Development Center, P.O. Box B, Frederick, MD 21702. e-mail: tessarol@ncifcrf.gov.

<sup>§</sup>Present address: Department of Neurological Surgery and The Miami Project, University of Miami School of Medicine, Miami, FL 33136.

<sup>\*\*</sup>Present address: The University of Texas, Southwestern Medical Center, Dallas, TX 75235.

The publication costs of this article were defrayed in part by page charge payment. This article must therefore be hereby marked "advertisement" in accordance with 18 U.S.C. §1734 solely to indicate this fact.

© 1997 by The National Academy of Sciences 0027-8424/97/9414776-6\$2.00/0  
PNAS is available online at <http://www.pnas.org>.

characterized mice with a targeted mutation that disrupts the expression of all *trkC* receptor proteins including the truncated isoforms (*trkC*  $-/-$ ). These *trkC*  $-/-$  mice exhibit the same abnormal posture and limb movements as the *trkC*-kinase  $-/-$  mice previously described (32). However, neuronal counts on neural crest and placode-derived sensory ganglia revealed that the losses of neurons were more severe in the *NT-3*  $-/-$  mice than in the *trkC*  $-/-$  animals described here. Furthermore, these *trkC*  $-/-$  mice exhibit more severe neuronal losses than those reported for the *trkC*-kinase  $-/-$  animals. Our findings suggest a function for the truncated *trkC* isoforms *in vivo* and strongly suggest that NT-3 also activates other "nonpreferred" *trk* receptors during development.

Most of the *trkC*  $-/-$  mice, like the *NT-3*  $-/-$  mice, die within the first week of birth. Histological examination of *trkC*-deficient mice unveiled a nonneuronal function for the *trkC* gene. *trkC*  $-/-$  mice exhibit a cardiac phenotype similar to the *NT-3*  $-/-$  animals (37), suggesting that the *trkC* receptor is the main transducer of NT-3 signaling to support the normal development of the mammalian heart.

## MATERIALS AND METHODS

**Targeting Vector and Generation of *trkC* Mutant Mice.** The replacement-type targeting vector consisting of a 9.0-kb 129/SV (Stratagene) mouse genomic fragment, where the exon containing the translation start codon, common to all isoforms, of the *trkC* locus was replaced with the pGK-neoBP cassette used as a positive selectable marker. The pGK-thymidine kinase cassette was introduced as negative selectable marker (Fig. 1*a*). Electroporation and selection were performed by using the CJ7 embryonic stem (ES) cell line (129/sv) as described (38). Genomic DNA derived from G418/FIAU-resistant ES cell clones were screened by using a diagnostic *EcoRV* restriction enzyme digestion with the 5' and 3' probes external to the targeting vector sequence indicated in Fig. 1*b*. Recombinant clones containing the expected 16-kb rearrangement were obtained at a frequency of 1/17.

Three independent *trkC* recombinant ES cell clones injected into C57BL/6 blastocysts generated chimeras that transmitted the mutated *trkC* allele to the progeny when mated to C57BL/6 females. Breeding of two *trkC*  $+/-$  mice gave rise to homozygous mutant mice at a frequency of 25%. Mice were bred in a specific, pathogen-free facility with food and water *ad libitum*.

**Western Blot Analysis.** Glycoproteins were concentrated from Nonidet P-40 lysates of mouse brains with wheat germ agglutinin-Sepharose, resolved on 7% SDS/PAGE, transferred to nitrocellulose, and detected with the antiserum 656 directed against the juxtamembrane domain of the *trkC* receptor as described (39).

**Histologic Techniques.** Heterozygote ( $+/-$ ) *NT-3* (35) or ( $+/-$ ) *trkC* mice were intercrossed by brother/sister matings for histological analysis of pups. The genotype of each newborn mouse was determined by analysis of tail-derived DNA as described (ref. 35; see above). Following decapitation, the bodies and heads of the newborn pups were immediately fixed in Bouin's fixative overnight. The next day after rinsing for few hours in water the heads and spinal cords were transferred to 70% ethanol and processed for paraffin embedding. The contents of the thoracic cavity were dissected en block prior to embedding in paraffin. For histological examination of the hearts, sections of 5  $\mu$ m were stained by using hematoxylin/eosin as described (40). For neuronal counts, the heads of one mutant and one wild-type littermate were embedded in the same block, sectioned sagittally at 5  $\mu$ m, and Nissl-stained with 0.1% cresyl violet. To assure unbiased analysis, neuronal counts were performed in a blinded fashion.

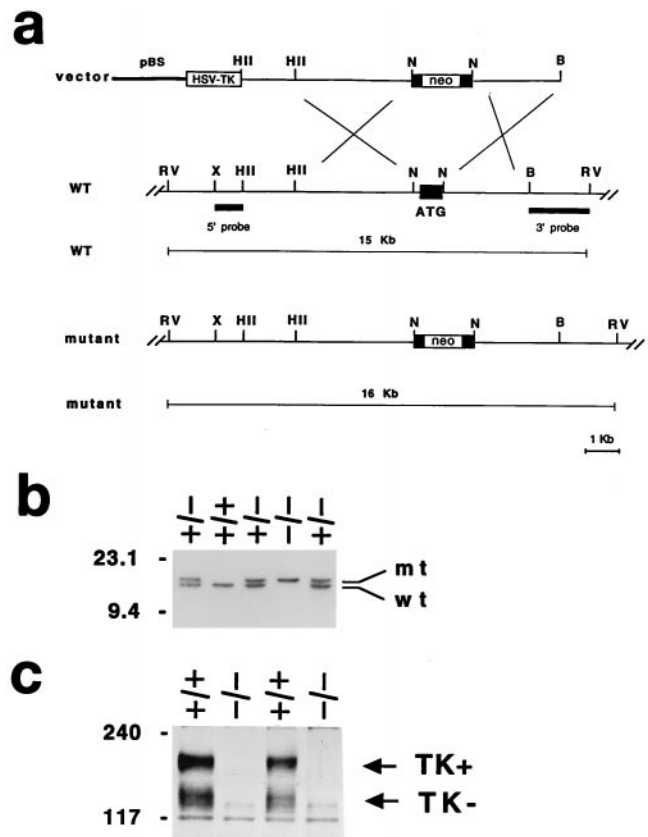


Fig. 1. Generation of *trkC*-deficient mice. (*a*) Schematic showing the replacement vector and strategy used to inactivate the *trkC* locus. Closed bar (ATG) indicates the *trkC* exon containing the translation start site. Restriction enzyme sites are as indicated. B, *Bam*HI; RV, *EcoRV*; X, *Xba*I; HII, *Hind*II; N, *Not*I. pBS indicates the pBluescript cloning vector (Stratagene). (*b*) Southern blot analysis of tail DNA from a litter obtained by intercrossing two *trkC*  $+/-$  mice. *EcoRV* restriction enzyme digestion and the 3' probe indicated in *a* were employed to detect rearrangements in the mouse *trkC* locus. The 15-kb wild-type (wt) and 16-kb rearranged (mt) DNA fragments are indicated; the positions of DNA molecular size markers are indicated on the left. (*c*) Western blot analysis of *trkC* protein expression in mutant ( $-/-$ ) and control ( $+/+$ ) newborn mouse brains. An antiserum directed against the juxtamembrane domain of the *trkC* receptor was employed for the analysis. The position of the full-length (TK $+$ ) and of the truncated (TK $-$ ) *trkC* proteins are indicated (arrows). Apparent molecular weights are indicated on the left.

## RESULTS

**Generation of *trkC*-Deficient Mice.** To disrupt all the isoforms encoded by the *trkC* locus, we constructed a vector in which part of the exon containing the translation start (ATG) codon was removed and replaced with the *neo* gene used as selectable marker (Fig. 1*a*). The resultant targeted allele was identified by Southern blot analysis (Fig. 1*b*). Western blot analysis of protein extracts from *trkC* mutant mouse brains confirmed the complete disruption of the *trkC* locus because both full-length and truncated isoforms could not be detected by an antibody specific for the common juxtamembrane domain of the *trkC* proteins (Fig. 1*c*). Furthermore, we did not detect any *trkC* mRNA by reverse transcription-PCR analysis (data not shown).

Mutant mice obtained by mating mice heterozygous for either the *trkC* or the *NT-3* (35) targeted mutation were scored for their survival rate (Fig. 2). Both *trkC*- and *NT-3*-deficient mice were generated in the same genetic strain background (129/C57bl/6) and maintained in the same facility under identical conditions. No significant differences in litter size

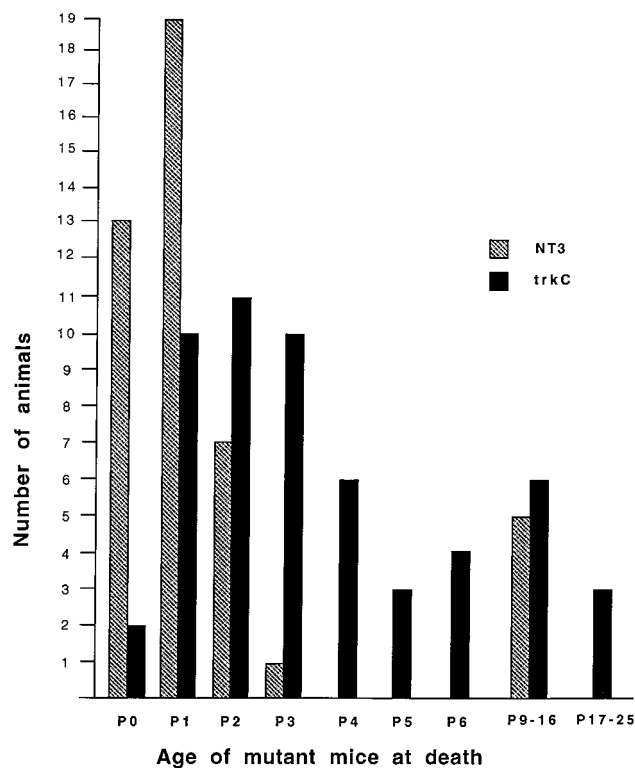


FIG. 2. Survival rate of *NT-3* and *trkC* mutant mice. Bar chart indicating the number of *NT-3* and *trkC* null mice that died at the specific age indicated (P, postnatal day). No mutant animal lived longer than 25 days.

were detected between the two mouse lines. However, there were significant differences in life span of 55 *trkC*  $-/-$  and 44 *NT-3*  $-/-$  mice. As shown in Fig. 2, 30% of *NT-3*  $-/-$  mice die immediately after birth whereas less than 5% of *trkC* mutant mice succumb in the first few hours postnatally. Furthermore, almost 90% of the *NT-3* knockout mice die by postnatal day 2 (P2), whereas equivalent lethality in *trkC* mutant mice is not reached until postnatal day 6 (P6) (Fig. 2). To further ensure uniformity of conditions, mutant mice were also obtained by mating mice heterozygous in both the *trkC*  $+/-$  and *NT-3*  $+/-$  locus. Similar to the data in Fig. 2, *NT-3* mutant mice showed reduced survival compared with their *trkC*  $-/-$  littermates (data not shown). Thus, mice lacking all *trkC* isoforms live slightly longer than the *NT-3*  $-/-$  ones. However, *trkC*  $-/-$  display a more severe phenotype than the *trkC*-kinase  $-/-$  animals that retain expression of the truncated isoforms and that live up to 4 weeks (32). Considering that both mutations were derived in a similar genetic background (129/C57bl/6), these results suggest that truncated *trkC* receptors may play a role in mouse development.

***NT-3*  $-/-$  Mice Exhibit a More Severe Loss of Sensory Neurons than *trkC*  $-/-$  Mice.** Mice lacking all *trkC* receptors display the same behavioral phenotype attributed to defects in proprioception observed in mice lacking either the full-length *trkC* tyrosine kinase receptors or *NT-3* (32–36). Retrograde labeling of sensory and motor neurons by using the lipid-soluble fluorescent tracer DiI in axial muscle at the lumbar level of *trkC* mutant mice confirmed the loss of Ia proprioceptive neuronal fibers that terminate in lamina IX of the spinal cord where they contact motor neurons to form the reflex arc (ref. 35; data not shown). Previous reports showed a reduced neuronal loss in the DRG of the *trkC*-kinase  $-/-$  mice relative to the ligand *NT-3*-deficient mice (32, 41). However, neuronal cell counts of other sensory ganglia from *trkC*-kinase  $-/-$  mice were not reported.

To rule out differences in neuronal cell counts caused by genetic background and/or methodology of analysis, we evaluated in parallel the *trkC*  $-/-$  and *NT-3*  $-/-$  mutant mice for loss of peripheral sensory and sympathetic neurons (Table 1). Neuronal cell counts of six different sensory ganglia were performed on individual newborn animals to allow direct comparisons also with the other neurotrophin and *trk* receptor knockouts that have been published recently (28, 29, 34, 42). As shown in Table 1, we confirmed the severe neuronal losses in the different sensory ganglia of *NT-3*  $-/-$  mice including the DRG at L5 level, trigeminal, cochlear, vestibular, geniculate, and petrosal-nodose. For example, we observed a 69% loss in L5 DRGs consistent with previous reports (33, 34). In the same ganglia the *trkC*  $-/-$  mice revealed less severe neuronal losses (33% in L5); yet, this reduction is significantly higher than that reported previously for the *trkC*-kinase  $-/-$  animals (17%) at P1 (41). Similarly, we observed a more severe neuronal loss in the cochlear ganglia of the *trkC*  $-/-$  mice ( $\approx 70\%$ ) relative to the *trkC*-kinase  $-/-$  animals (51%; ref. 41). Yet, we confirmed the severe loss (87%) reported for the *NT-3*  $-/-$  mice (85%; refs. 33 and 34). However, some ganglia demonstrated similar losses in the *trkC*  $-/-$  and the *trkC*-kinase  $-/-$  mice. In the trigeminal ganglia, reduction by 20% is noted in both lines and in the vestibular ganglia similar neuronal losses of  $\approx 15\%$  are found (refs. 41 and 43; Table 1). Taken together, these data suggest that the truncated *trkC* isoform may play a role, at least in certain sensory ganglia. However, unless a direct comparison between the two mutant animals is performed, it is difficult to discern if the differences observed are significant and not caused by the criteria used for counting neurons or are caused by the presence of nontyrosine kinase forms of *trkC*.

Information on neuronal cell counts in the geniculate and petrosal-nodose ganglia have not been published for the *trkC*-kinase  $-/-$  mice. However, comparisons can be made with the *NT-3*  $-/-$  mice (Table 1). Significant differences in

Table 1. Neuronal cell counts in sensory and sympathetic populations of wild type, *trkC*, and *NT-3* mutant mice

	Wild type (5)	<i>trkC</i> $-/-$ (5)	Reduction, %
Sensory ganglia			
Trigeminal	50,646 $\pm$ 353	39,912 $\pm$ 638	21***
Geniculate	1,569 $\pm$ 132	1,419 $\pm$ 85	11
Vestibular	4,324 $\pm$ 106	3,668 $\pm$ 60	15***
Cochlear	8,761 $\pm$ 644	2,611 $\pm$ 162	70***
Petrosal-nodose	10,084 $\pm$ 353	8,659 $\pm$ 296	14***
L5 dorsal root (3)	7,157 $\pm$ 587	4,770 $\pm$ 337	33**
Sympathetic ganglion			
Superior cervical (3)	25,084 $\pm$ 2,140	25,956 $\pm$ 1,912	0
	Wild type (3)	<i>NT-3</i> $-/-$ (3)	Reduction, %
Sensory ganglia			
Trigeminal	39,765 $\pm$ 1,334	14,808 $\pm$ 953	62***
Geniculate	1,465 $\pm$ 135	949 $\pm$ 85	35*
Vestibular	4,110 $\pm$ 335	3,352 $\pm$ 325	19
Cochlear	7,905 $\pm$ 331	980 $\pm$ 270	87***
Petrosal-nodose	9,724 $\pm$ 1,118	6,396 $\pm$ 724	34**
L5 dorsal root	7,107 $\pm$ 627	2,222 $\pm$ 173	69***
Sympathetic ganglion			
Superior cervical	23,862 $\pm$ 1,550	13,578 $\pm$ 1,896	44***

Tissue sections of newborn (P0) wild type and mutant littermates were prepared as described. Neurons having a clear nucleus and nucleolus were counted in every sixth section, and the sum of counts was multiplied by 6. Values are not corrected and are expressed as mean number of neurons  $\pm$  SEM. Differences were evaluated using a one-tailed Student's test; \* $P < 0.01$ , \*\* $P < 0.02$ , \*\*\* $P < 0.005$ . In parenthesis, the numbers of animals analyzed are indicated. Wild-type mice derived from intercrosses of heterozygous *trkC* or *NT-3* mice showed a significant difference in neuronal counts of the trigeminal ganglion. We hypothesize that this is caused by a maternal effect of reduced circulating *NT-3* in the pregnant *NT-3*  $+/-$  mice.



reduction of neurons in both geniculate and petrosal-nodose neuronal losses were noted between the *NT-3*<sup>-/-</sup> mice (35% and 34%) and the *trkC*<sup>-/-</sup> mice (11% and 14%).

We also evaluated the superior cervical ganglion, because *NT-3* is known to play an important role in its development and can support sympathetic neuroblasts *in vitro* (33, 34, 44, 45). At early stages of development, only *trkC* is expressed in this ganglion (46). At later stages, postmitotic neurons express *trkA* and require *NGF* as a target derived neurotrophin (46, 47). Considering the mediation of *NT-3* activity by *trkC* in early sympathetic neuroblasts, we expected to see similar neuronal losses in *NT-3*<sup>-/-</sup> and *trkC*<sup>-/-</sup> mice ( $\approx 50\%$ ). However, as reported for *trkC*-kinase<sup>-/-</sup> mice (46), we did not see any reduction at all in *trkC*<sup>-/-</sup> mice (Table 1). These data support the notion that, *in vivo*, *NT-3* might act at later stages of sympathetic ganglion development through *trkA*. Furthermore, a recent report showed that *trkC*-kinase<sup>-/-</sup> sympathetic neurons in culture can be rescued by adding *NT-3* to the culture media (48). Although saturating amounts of the neurotrophin were used in this experiment, this data also suggested that *NT-3* can act through other receptors during neuronal development.

**Cardiac Defects in *trkC*-Deficient Mice.** In rodents, neurotrophins and their receptors are expressed in many developing organs. In particular, the presence of both *NT-3* and *trkC* mRNAs has been reported in the heart, the aorta and putative migrating neural crest cells (23, 31, 40, 49, 50). Recently, we have shown that mice lacking *NT-3* have severe defects in cardiac structures of neural crest origin including atrial and ventricular dilatation, atrial and ventricular septal defects, and abnormalities of valvular architecture (37). To establish whether the defects found in the *NT-3*<sup>-/-</sup> mouse are caused by a failure in activating the *trkC* receptor, we analyzed the hearts of eight *trkC*-deficient mice.

Examination of the thoracic cavity of these animals revealed markedly enlarged and globular hearts with congested, hemorrhagic lungs. Microscopic evaluation displayed valvular defects in all animals, with hypertrophy/hyperplasia of the pulmonary valve occurring most frequently (3/8 of the *trkC*<sup>-/-</sup> animals; Table 2; Fig. 3 *e* and *f*). In addition, there was hypertrophy and thickening of the pulmonary veins as they branch within the lung parenchyma. Defects in chamber septation were detected in the majority of the animals with 4/8 demonstrating large atrial secundum defects, and 3/8 with large ventricular septal defects (Fig. 3 *a-d*). Abnormalities in the development or septation of the cardiac outflow tracts were also noted, with the identification of one animal with an apparent truncus arteriosus (incomplete septation of the aorta and pulmonary artery). All animals exhibited significant right ventricular chamber enlargement, although this may represent a secondary defect given the severity of associated valvular and septa abnormalities (Table 2).

The frequency, severity, and type of cardiovascular defects in the *trkC*<sup>-/-</sup> animals are similar to those described in the *NT-3*<sup>-/-</sup> animals (37). These results suggest that *trkC* mediates most *NT-3* signaling in cardiac development. Furthermore, the presence of *trkC* receptors in neural crest cells migrating during embryogenesis and the identification of

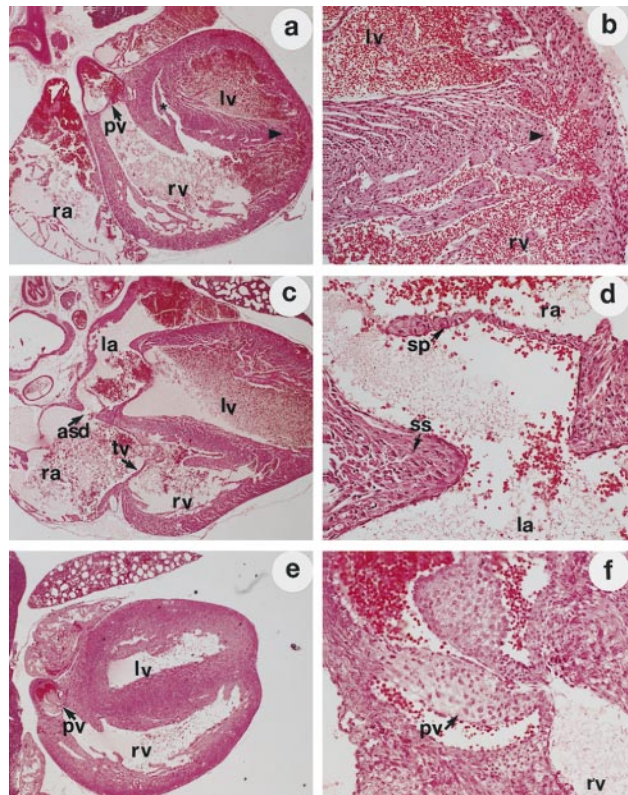


FIG. 3. Malformations in cardiogenesis of *trkC*<sup>-/-</sup> mice. Representative hematoxylin/eosin stained sections of newborn *trkC*<sup>-/-</sup> mice (P0). The genotype of each animal was determined by Southern blot analysis. (a) Section of a heart demonstrating ventricular septal defects (\* and arrowhead). ( $\times 25$ .) (b) Higher magnification ( $\times 75$ ) of *a*, with ventricular septal defect (arrowhead) indicated. (c) Atrial septal defect (asd) in a *trkC*<sup>-/-</sup> mouse heart. (d) Higher magnification ( $\times 75$ ) of *c* with septum primum (sp) and septum secundum (ss) indicated. (e) Section demonstrating thickening of pulmonary valve leaflets (pv). ( $\times 25$ .) (f) Higher magnification of *e* ( $\times 75$ ), with thickening of pulmonary valve leaflet indicated. rv, Right ventricle; lv, left ventricle; pv, pulmonary valve; tv, tricuspid valve; ra, right atrium; la, left atrium.

cardiac defects in structures of neural crest origin is consistent with a direct role for *trkC* in the cardiac neural crest migration (23, 37).

## DISCUSSION

*In vitro* experiments have demonstrated that *NT-3* activates most effectively the *trkC* receptor tyrosine kinase, but it can also signal through *trkA* and *trkB* under certain experimental conditions (13). Whether these interactions occur also *in vivo* and have physiological relevance is unresolved (51). The availability of *trk* and neurotrophin null mutant mice has provided a tool to investigate the significance of these ligand/receptor interactions *in vivo*. *NT-3*-deficient mice have been independently generated by several laboratories. Mice lacking the kinase active isoforms of *trkC* have been reported by Klein and colleagues (32) who observed a less severe phenotype in these mice compared with *NT-3* null animals (41, 51). To date, it has been unclear whether this discrepancy was caused by the presence of the noncatalytic isoforms of the *trkC* receptor. Thus, we have generated mice that lack expression of all the kinase active and truncated isoforms of *trkC*. The present study is a direct comparison of neuronal deficits in mice lacking either the ligand *NT-3* or the receptor *trkC*. We have confirmed previously published reports on neuronal cell losses in both sensory and sympathetic neuronal populations of *NT-3*

Table 2. Heart abnormalities in *trkC*-deficient animals

Defects	<i>trkC</i> <sup>-/-</sup>	Wild type
Globular heart	8/8	0/6
ASD	4/4	0/6
VSD	3/8	0/6
Pulmonic stenosis	3/8	0/6
Truncus arteriosus	1/8	0/6
Valvular defects (AV, MV, TV, PV)	8/8	0/6

ASD, atrial septal defect; VSD, ventricular septal defects; AV, aortic valve; MV, mitral valve; TV, tricuspid valve; PV, pulmonic valve.

null mice (33, 34). Furthermore, we obtained similar neuronal cell counts in trigeminal, vestibular, and superior cervical ganglia as have been reported for mice lacking only kinase active *trkC* isoforms (41, 46, 48). However several significant differences were observed: *trkC*  $-/-$  mice live significantly shorter than *trkC*-kinase  $-/-$  mice, although both lines were generated in the same genetic background (32); neuronal cell losses in ganglia such as vestibular and DRGs were more severe in *trkC*  $-/-$  deficient mice. These differences suggest that, in mouse, truncated *trkC* receptors play a role in the development of subpopulations of sensory neurons and possibly other structures.

At least one isoform of the truncated *trkC* receptors has an intracellular domain that is highly conserved between mammals and birds, suggesting a signaling function, as a docking site for proteins within a signal transduction pathway involved in neurogenesis (30, 31, 52). However, the truncated isoform(s) could also have roles in sequestering ligand or in regulating full length receptor functions by forming heterodimers of truncated and kinase active *trkC* isoforms in the presence of the ligand. These later hypotheses are supported by our recent finding that mice which overexpress a truncated isoform of the *trkC* receptor develop a phenotype similar to the *NT-3*  $-/-$  mice. These results suggest that the receptor could sequester NT-3 or act in a dominant negative manner to suppress signaling by the kinase active *trkC* isoforms (M.E.P. and L.T., unpublished data). Other studies investigating the role of truncated *trkB* receptors support such ideas. In particular, the expression pattern of a truncated *trkB* receptor in the chicken developing inner ear suggests that truncated *trkB* molecules form an efficient and selective barrier preventing the diffusion of BDNF and eliminating it by internalization (53). Furthermore, truncated *trkB* receptors expressed in *Xenopus* oocytes, function as dominant negative in a heterodimer with the full-length isoform inhibiting the BDNF signaling (54).

Regardless of the differences observed between mice lacking all *trkC* receptors or only the kinase active isoforms, both lines display significantly less severe neuronal cell losses in almost all ganglia compared with the defects in *NT-3*  $-/-$  animals. Thus, our data strongly support the notion that NT-3 acts also through other *trk* receptors in neuronal development.

In particular, we found a 70% reduction of DRG neurons at P0 in *NT-3*-deficient mice, whereas *trkC*  $-/-$  mice are missing only 33% of these neurons. Other groups have studied extensively the embryonic DRG of *NT-3*  $-/-$  mice and proposed that in these embryos the precursors cells at embryonic day (E) 11 to E12 undergo apoptosis, accounting for the 70% neuronal cell losses (55). Because only a fraction of DRG neurons are missing in *trkC* mutant mice, it has been suggested that NT-3 could support DRG neurons by activating *trkA* or *trkB*, although this effect could be artificial because of the absence of *trkC* (51). White *et al.* (51) proposed that as the onset of survival-dependence on NGF and *trkA* signaling is concurrent and of equal magnitude at E13.5, NT-3 alone could not support DRG neurons via *trkA* in the wild-type embryo. However, a recent study by Fariñas *et al.* (57) provides a more complicated scenario for survival-dependence of early DRG neurons. At E11, they observe an increase in apoptosis of DRG neurons in *NT-3* null mutant mice, and suggest that these could be proprioceptive neurons, because they are formed first in the DRG (56). At E12 in the DRGs of *NT-3*  $-/-$  mice, the precursor cells display proliferation and survival rates that match those of wild-type animals. Furthermore, there is a dramatic increase in the accumulation of neurons in the ganglia of *NT-3* mutant animals, suggesting that lack of NT-3 causes precursors cells to prematurely exit the cell cycle. Prematurely differentiated neurons would then undergo massive cell death at E12–13 (51, 57). Thus, contrary to the report by ElShamy and Ernors (55), Fariñas *et al.* (57) suggest that

neurons and not precursor cells undergo apoptosis. These authors also suggest that there are several temporal waves of neurogenesis in the DRG. The first population of cells affected in the *NT-3*  $-/-$  mice at E11 could be *trkC*-expressing neurons (proprioceptive). The second population affected in the *NT-3*  $-/-$  animals at E12–E13 might express a *trk* receptor other than *trkC*. NT-3 can activate *trkA* in certain cellular backgrounds and is produced by the mesenchyme surrounding the DRGs by E11–E12 (13, 57). In addition, local concentrations of NT-3 could reach levels sufficient to activate *trkA* expressed in neuronal cells. Lastly, a population of DRG neuron at E11.5 express the *trkA* receptor and could represent the second population affected in the *NT-3*  $-/-$  mice (35, 51). In view of these considerations and our current results, we suggest that NT-3 activates the *trkA* receptor *in vivo*. However, such an effect may be restricted to a specific developmental stage of the DRG.

We and others have reported expression of neurotrophins, and their cognate *trk* receptors, in the vascular system (23, 40, 49, 50, 58). Recently, we have shown that *NT-3*-deficient mice exhibit severe cardiac abnormalities including atria and ventricular septa defects and abnormal valvular architecture. Furthermore, we have observed decreased levels of *trkC* expression in the hearts of *NT-3*  $-/-$  embryos, suggesting that the absence of *NT-3* expression could result in a reduction of *trkC* expressing populations within the developing cardiovascular system (37). Our current findings show that the *trkC*  $-/-$  animals have cardiac abnormalities similar to the ones identified in the *NT-3*  $-/-$  mice. Thus, these defects establish *trkC* as the most likely transducer of NT-3 action in heart development. The cardiac defects in both null mutant mice involve structures of neural crest origin indicating that NT-3 and *trkC* are essential for regulating the development of cardiac neural crest. Further studies of embryonic stages will be required to determine whether NT-3/*trkC* signaling regulates the migration, proliferation, and/or survival of the neural crest cells. Furthermore, the results suggest that in cardiac crest development, NT-3 does not function effectively through less preferred *trk* receptors, *trkA* or *trkB*.

The *trkC*-deficient mice have a less severe neuronal phenotype than *NT-3*-deficient mice, and to date we have not established whether there are differences in the cardiac innervation between the two lines. More specific analysis will address this issue and may identify this mouse as an animal model complementary to the *NT-3*  $-/-$  for the study of human cardiac congenital abnormalities.

We thank Marie Mazzulla, Susan Reid, James Resau, and Eric Klineberg for excellent technical assistance; Isabel Fariñas and Luis Reichardt for sharing their unpublished results; and Esta Sterneck for critical reading of the manuscript. This work was supported by the National Cancer Institute, under contract with ABL (L.T., P.T., L.F.P., J.B.F., and M.E.P.), and by the New York Heart Association and the Hirschl-Weill/Caullier Trust (B.L.H.). B.L.H. is an Established Investigator of the American Heart Association.

- Lewin, G. R. & Barde, Y.-A. (1996) *Annu. Rev. Neurosci.* **19**, 289–317.
- Barde, Y.-A. (1990) *Prog. Growth Factor Res.* **2**, 237–248.
- Gotz, R., Koster, R., Winkler, C., Raulf, F., Lottspeich, F., Schartl, M. & Thoenen, H. (1994) *Nature (London)* **372**, 266–269.
- Perez, P., Coll, P. M., Hempstead, B. L., Martin-Zanca, D. & Chao, M. V. (1995) *Mol. Cell. Neurosci.* **6**, 97–105.
- Urfer, R., Tsoulfas, P., O'Connell, L., Shelton, D. L., Parada, L. F. & Presta, L. G. (1995) *EMBO J.* **14**, 2795–2805.
- Greene, L. A. & Kaplan, D. R. (1995) *Curr. Opin. Neurobiol.* **5**, 579–587.
- Chao, M. V. & Hempstead, B. L. (1995) *Trends Neurosci.* **18**, 321–326.
- Kaplan, D. R., Hempstead, B. L., Martin-Zanca, D., Chao, M. V. & Parada, L. F. (1991) *Science* **252**, 554–558.



9. Soppet, D., Escandon, E., Maragos, J., Middlemas, D. S., Reid, S. W., Blair, J., Burton, L. E., Stanton, B. R., Kaplan, D. R., Hunter, T., Nikolics, K. & Parada, L. F. (1991) *Cell* **65**, 895–903.
10. Klein, R., Nanduri, V., Jing, S., Lamballe, F., Tapley, P., Bryant, S., Cordon-Cardo, C., Jones, K. R., Reichardt, L. F. & Barbacid, M. (1991) *Cell* **66**, 395–403.
11. Klein, R., Lamballe, F., Bryant, S. & Barbacid, M. (1992) *Neuron* **8**, 947–956.
12. Lamballe, F., Klein, R. & Barbacid, M. (1991) *Cell* **66**, 967–979.
13. Ip, N. Y., Stitt, T. N., Tapley, P., Klein, R., Greene, L. A., Barbacid, M. & Yancopoulos, G. D. (1993) *Neuron* **10**, 137–149.
14. Merlio, J.-P., Ernfors, P., Jaber, M. & Persson, H. (1992) *Neuroscience* **51**, 513–532.
15. Schecterson, L. C. & Bothwell, M. (1992) *Neuron* **9**, 449–463.
16. Mu, X., Silos-Santiago, I., Carrol, S. & Snider, W. D. (1993) *J. Neurosci.* **13**, 4029–4041.
17. McMahon, S. B., Armanini, M. P., Ling, L. H. & Phillips, H. S. (1994) *Neuron* **12**, 1161–1171.
18. Davies, A. M. (1994) *J. Neurobiol.* **25**, 1334–1348.
19. Buchman, V. L. & Davies, A. M. (1993) *Development (Cambridge, U.K.)* **118**, 989–1001.
20. Paul, G. & Davies, A. M. (1995) *Dev. Biol.* **171**, 590–605.
21. Kokaia, Z., Bengzon, J., Metsis, M., Kokaia, M., Persson, H. & Lindvall, O. (1993) *Proc. Natl. Acad. Sci. USA* **90**, 6711–6715.
22. Miranda, R. C., Sohrabji, F. & Toran-Allerand, C. D. (1993) *Proc. Natl. Acad. Sci. USA* **90**, 6439–6443.
23. Tessarollo, L., Tsoulfas, P., Martin-Zanca, D., Gilbert, D. J., Jenkins, N. A., Copeland, N. & Parada, L. F. (1993) *Development (Cambridge, U.K.)* **118**, 463–475.
24. Smeyne, R. J., Klein, R., Schnapp, A., Long, L. K., Bryant, S., Lewin, A., Lira, S. A. & Barbacid, M. (1994) *Nature (London)* **368**, 246–248.
25. Jones, K. R., Fariñas, I., Backus, C. & Reichardt, L. F. (1994) *Cell* **76**, 989–999.
26. Klein, R., Smeyne, R. J., Wurst, W., Long, L. K., Auerbach, B. A., Joyner, A. L. & Barbacid, M. (1993) *Cell* **75**, 113–122.
27. Ernfors, P., Lee, K.-F. & Jaenisch, R. (1994) *Nature (London)* **368**, 147–150.
28. Liu, X., Ernfors, P., Wu, H. & Jaenisch, R. (1995) *Nature (London)* **375**, 238–241.
29. Conover, J. C., Erickson, J. T., Katz, D. M., Bianchi, L. M., Poueymirou, W. T., McClain, J., Pan, L., Helgren, M., Ip, N. Y., Boland, P., Friedman, B., Wiegand, S., Vejsada, R., Kato, A. C., DeChiara, T. M. & Yancopoulos, G. D. (1995) *Nature (London)* **375**, 235–238.
30. Valenzuela, D. M., Maisonpierre, P. C., Glass, D. J., Rojas, E., Nuñez, L., Kong, Y., Gies, D. R., Stitt, T. N., Ip, N. Y. & Yancopoulos, G. D. (1993) *Neuron* **10**, 963–974.
31. Tsoulfas, P., Soppet, D., Escandon, E., Tessarollo, L., Mendoza-Ramirez, J.-L., Rosenthal, A., Nikolics, K. & Parada, L. F. (1993) *Neuron* **10**, 975–990.
32. Klein, R., Silos-Santiago, I., Smeyne, R. J., Lira, S. A., Brambilla, R., Bryant, S., Zhang, L., Snider, W. D. & Barbacid, M. (1994) *Nature (London)* **368**, 249–251.
33. Ernfors, P., Lee, K.-F., Kucera, J. & Jaenisch, R. (1994) *Cell* **77**, 503–512.
34. Fariñas, I., Jones, K. R., Backus, C., Wang, X.-Y. & Reichardt, L. F. (1994) *Nature (London)* **369**, 658–661.
35. Tessarollo, L., Vogel, K. S., Palko, M. E., Reid, S. W. & Parada, L. F. (1994) *Proc. Natl. Acad. Sci. USA* **91**, 11844–11848.
36. Tojo, H., Kaisho, Y., Nakata, M., Matsuoka, K., Kitagawa, M., Abe, T., Takami, K., Yamamoto, M., Shino, A., Igarashi, K., Aizawa, S. & Shiho, O. (1995) *Brain Res.* **669**, 163–175.
37. Donovan, M. J., Hahn, R., Tessarollo, L. & Hempstead, B. L. (1996) *Nat. Genet.* **14**, 210–213.
38. Swiatek, P. J. & Gridley, T. (1993) *Genes Dev.* **7**, 2071–2084.
39. Tsoulfas, P., Stephens, R. M., Kaplan, D. R. & Parada, L. R. (1996) *J. Biol. Chem.* **271**, 5691–5697.
40. Donovan, M. J., Miranda, R. C., Kraemer, R., McCaffrey, T. A., Tessarollo, L., Mahadeo, D., Sharif, S., Kaplan, D. R., Tsoulfas, P., Parada, L. F., Toran-Allerand, C. D., Hajar, D. P. & Hempstead, B. L. (1995) *Am. J. Pathol.* **147**, 309–324.
41. Minichiello, L., Piehl, F., Vasquez, E., Schimmang, T., Hökfelt, T., Represa, J. & Klein, R. (1995) *Development (Cambridge, U.K.)* **121**, 4067–4075.
42. Snider, W. D. (1994) *Cell* **77**, 627–638.
43. Pinon, L. G., Minichiello, L., Klein, R. & Davies, A. M. (1996) *Development (Cambridge, U.K.)* **122**, 3255–3261.
44. Birren, S. J., Lo, L. & Anderson, D. J. (1993) *Development (Cambridge, U.K.)* **119**, 597–610.
45. DiCicco-Bloom, E., Friedman, W. J. & Black, I. B. (1993) *Neuron* **11**, 1101–1111.
46. Fagan, A. M., Zhang, H., Landis, S., Smeyne, R. J., Silos-Santiago, I. & Barbacid, M. (1996) *J. Neurosci.* **16**, 6208–6218.
47. Levi-Montalcini, R. & Booker, B. (1960) *Proc. Natl. Acad. Sci. USA* **46**, 384–391.
48. Davies, A. M., Minichiello, L. & Klein, R. (1995) *EMBO J.* **14**, 4482–4489.
49. Scarisbrick, I. A., Jones, E. G. & Isackson, P. J. (1993) *J. Neurosci.* **13**, 875–893.
50. Hiltunen, J. O., Arumae, U., Moshnyakov, M. & Saarna, M. (1996) *Circ. Res.* **79**, 930–939.
51. White, F. A., Silos-Santiago, I., Molliver, D. C., Nishimura, M., Philips, H., Barbacid, M. & Snider, W. D. (1996) *J. Neurosci.* **16**, 4662–4672.
52. Garner, A. S. & Large, T. H. (1994) *Neuron* **13**, 457–472.
53. Biffo, S., Offenhauser, N., Carter, B. D. & Barde, Y. A. (1995) *Development (Cambridge, U.K.)* **121**, 2461–2470.
54. Eide, F. F., Vining, E. R., Eide, B. L., Zang, K., Wang, X.-Y. & Reichardt, L. F. (1996) *J. Neurosci.* **16**, 3123–3129.
55. ElShamy, W. M. & Ernfors, P. (1996) *Neuron* **16**, 963–972.
56. Lawson, S. N. & Biscoe, T. J. (1979) *J. Neurocytol.* **8**, 265–274.
57. Fariñas, I., Yoshida, C. K., Backus, C. & Reichardt, L. F. (1996) *Neuron* **17**, 1065–1078.
58. Lamballe, F., Smeyne, R. J. & Barbacid, M. (1994) *J. Neurosci.* **14**, 14–28.